Geophysical Research Letters®

Key Points:

- The pore-scale dynamics of multiphase flow in heterogeneous rocks were investigated using fast laboratory-based 4D X-ray microtomography
- We describe a pore-scale displacement mechanism with displacement rates orders of magnitude slower than those in neighboring pores
- We demonstrate that viscous forces could play a significant role even at very low global capillary numbers under mixed-wet conditions

Correspondence to:

A. Mascini,
Arjen.Mascini@UGent.be

Fluid Invasion Dynamics in Porous Media With Complex Wettability and Connectivity

Arjen Mascini[1,2] ![ORCID], **Marijn Boone[3], Stefanie Van Offenwert[1,2]** ![ORCID], **Shan Wang[1,2]** ![ORCID], **Veerle Cnudde[1,2,4]** ![ORCID], **and Tom Bultreys[1,2]** ![ORCID]

[1]Pore-scale Processes in Geomaterials Research Team (PProGRess), Department of Geology, Ghent University, Ghent, Belgium, [2]Centre for X-ray Tomography (UGCT), Ghent University, Ghent, Belgium, [3]TESCAN XRE, Ghent, Belgium, [4]Department of Earth Sciences, Utrecht University, Utrecht, The Netherlands

Abstract Multiphase flow is important for many natural and engineered processes in subsurface geoscience. Pore-scale multiphase flow dynamics are commonly characterized by an average balance of driving forces. However, significant local variability in this balance may exist inside natural, heterogeneous porous materials, such as rocks and soils. Here, we investigate multiphase flow in heterogeneous rocks with different wetting properties using fast laboratory-based 4D X-ray imaging. The mixed-wet dynamics were characterized by displacement rates that differed over orders of magnitude between directly neighboring pores. While conventional understanding predicted strongly capillary-dominated conditions, our analysis suggests that viscous forces played a key role in these dynamics, facilitated by a complex interplay between the mixed-wettability and the pore structure. These dynamics highlight the need for further studies on the fundamental controls on multiphase flow in geomaterials, which is crucial to design, for example, groundwater remediation and subsurface CO_2 storage operations.

Plain Language Summary The flow of multiple fluids through a porous material plays an important role in many industrial and natural processes such as rain infiltrating a dry soil or CO_2 storage in the subsurface. At the pore-scale, these flows are governed by forces which depend on the pore-geometry and the relative affinities of the fluids with the solid (i.e., wettability). The rates at which fluids flow in geological reservoirs is in most cases considered to be very slow (in the order of tens of meters per year). At these slow flow rates, fluid displacements are thought to be controlled by capillary forces. However, much of our current understanding of multiphase flow stems from artificial samples with simplified geometries, while most natural geomaterials tend to be far more complex in terms of pore structure and wettability. We show that heterogeneous pore structures and wetting properties can lead to different mechanisms of fluid displacement compared to those observed in model materials due to local variations in the viscous-capillary force balance. This implies that models commonly used to predict subsurface flow process such as geological CO_2 storage that assume capillary forces to dominate may not adequately capture the dynamics at the pore-scale.

1. Introduction

The simultaneous flow of multiple fluid phases through a porous material is an important process encountered in many natural and manmade systems. In earth sciences, it is critically important for the injection and safe storage of CO_2 in deep saline aquifers (Bui et al., 2018), geological energy storage (Mouli-Castillo et al., 2019) and the study of subsurface contaminant transport (Mercer & Cohen, 1990).

The pore-scale dynamics of multiphase flow in porous media are known to be governed by a competition between the driving forces on the fluids: capillary, viscous, inertial and gravitational forces (Chen et al., 2019; Holtzman, 2016; Hu et al., 2019; Lenormand et al., 1983; B. Zhao et al., 2016). These dynamics determine how fluids occupy the available space in the pores and how the resulting fluid distribution evolves over time. Fluid invasion in 2D networks was found to have qualitatively different properties when the injection flow rate or fluid properties were varied (Blunt & Scher, 1995; Lenormand et al., 1988), resulting in a "phase diagram" of flow regimes based on the capillary number (average ratio of viscous to capillary forces) and the ratio of the viscosity of the two fluids. The development of pore-scale fluid arrangements into distinct

patterns has a crucial impact on the macroscopic transport behavior, yet continues to challenge our pore-scale models (B. Zhao et al., 2019).

A particular problem has been the understanding of how pore-scale variations in the pore geometry and the wettability (the relative affinity of the fluids to the solid surface) affect fluid intrusion in porous materials. Recently, Lenormand's phase diagram was extended to incorporate random disorder (Holtzman, 2016) and the influence of homogeneous wetting conditions in 2.5D micro-models (Trojer et al., 2015; B. Zhao et al., 2016). The wettability was found to strongly influence the dominant displacement mechanisms during the invasion process. When the solid surfaces are non-wetting to the invading fluid (i.e., drainage) displacements happen as piston-like movements associated with Haines instabilities (Haines, 1930; Lenormand et al., 1983). In the opposite scenario (i.e., imbibition), flow through layers and corners has an important influence on the displacements (Lenormand & Zarcone, 1984). In intermediate wet conditions, cooperative-pore body filling plays an important role (Cieplak & Robbins, 1990).

Natural materials, such as porous rocks, sediments and soils, frequently exhibit much higher degrees of correlated disorder than micromodels, with pore sizes spanning many orders of magnitude (Blunt et al., 2013). Furthermore, the effective wettability in the pores of geological materials is subject to variations in mineral composition and surface roughness at all length scales (de Gennes, 1985; Morrow, 1975), and can be impacted by coatings of surface-active components, particularly in hydrocarbon reservoirs (Morrow, 1990) and polluted aquifers (Al-Raoush, 2009). This can lead to different surfaces having a different fluid affinity, commonly referred to as "mixed-wettability" (AlRatrout et al., 2018; Kovscek et al., 1992). The dynamics in mixed-wet materials can differ from those with uniform wetting as interfaces with both concave and convex shapes can co-exist while maintaining the connectivity of both fluids (Lin et al., 2019; Rabbani et al., 2017). Due to structural and wetting heterogeneities, multiphase flow has spatial dependencies that stretch over many pores, and consequently it is still poorly understood how pore-scale heterogeneities influence the fluid invasion dynamics.

To study the fluid invasion dynamics in complex porous media, time-resolved high resolution X-ray microtomography (mCT) can be applied to image the fluids' distribution in the pores at the second to minute timescale in three dimensions (Bultreys et al., 2016; Withers et al., 2021). This technique led to the first observations of capillary-dominated fluid displacement events in rock samples (Berg et al., 2013; Bultreys et al., 2015; Singh et al., 2017) and of complex dynamic effects, such as ganglion dynamics (Rücker et al., 2015) and intermittency (Reynolds et al., 2017). Despite this significant progress, most time-resolved imaging has been performed on rocks with essentially single-scale pore structures and uniform wettability. The dynamics of multiphase flow in samples with a mixed-wettability, but still with a simple pore structure, have only recently started to be studied (Rücker et al., 2019; Scanziani et al., 2020). Furthermore, most studies have focused on describing the geometry and connectivity of the fluids during displacements and in the resulting fluid distributions, while the timescales associated with the dynamics received relatively little attention (Schlüter et al., 2017). This leaves unanswered whether the current knowledge on capillary-dominated fluid dynamics covers the behavior that typically occurs in the subsurface.

In this work, the pore-scale dynamics of capillary-dominated multiphase flow are investigated in microcores of a heterogeneous sandstone in both homogeneously water-wet and mixed-wet conditions. The timescales of fluid displacements are estimated on a pore-by-pore basis using time-resolved laboratory-based X-ray mCT to image the fluid distribution in the pores. We show that the dynamics were qualitatively different for mixed-wet versus water-wet conditions. Under mixed-wet conditions, a significant fraction of the pores had fluid displacement timescales that were several orders of magnitude slower than directly neighboring pores. These slow dynamics appeared to be dominated by the fluid conductivity rather than by capillary forces (despite the low capillary number). This implies that viscous forces might play an important role in flow regimes commonly thought to be controlled by capillary forces. This puts into question the use of classical concepts such as the capillary number to characterize multiphase flow.
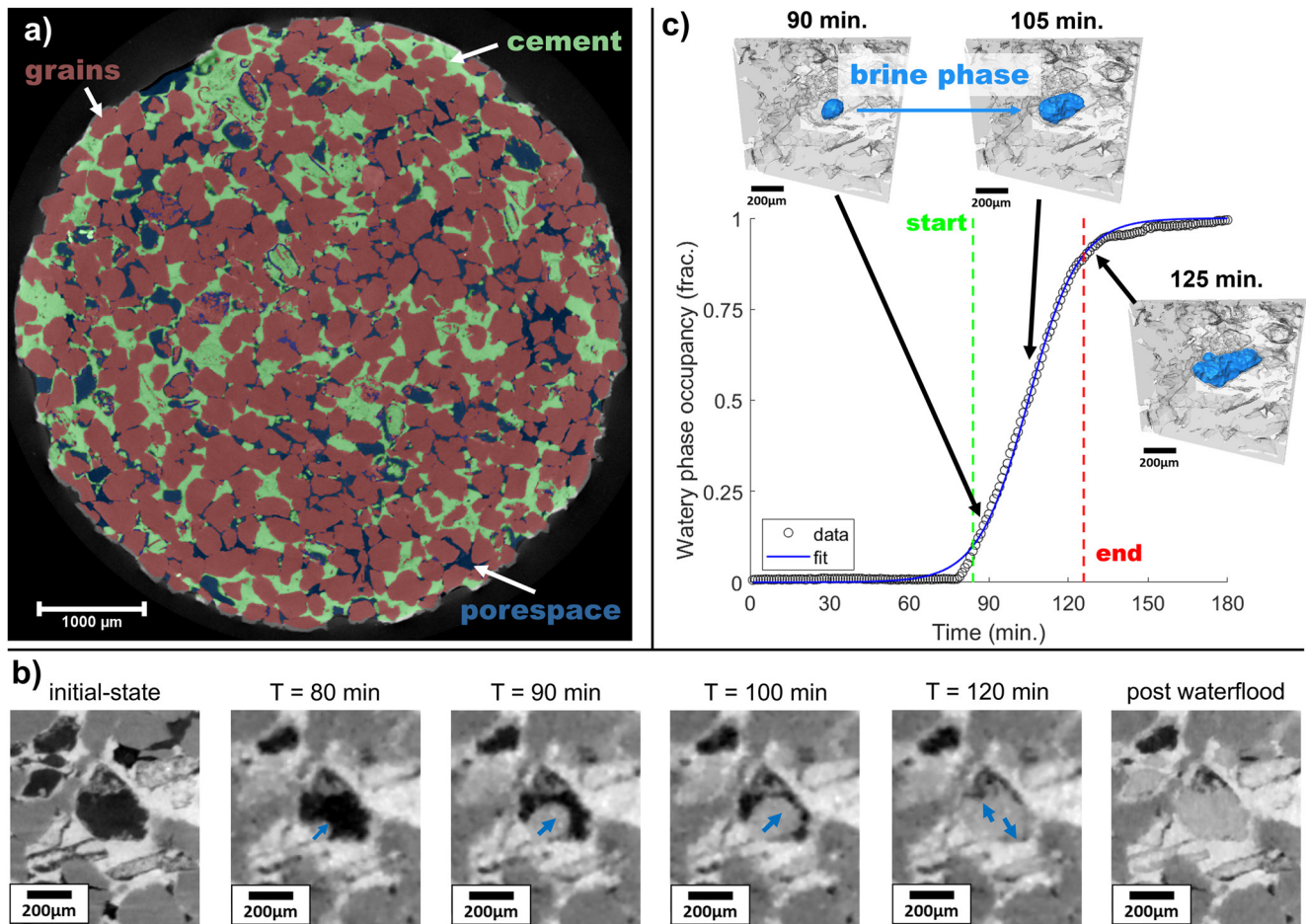
Figure 1. (a) 2D slice through the tomogram of the initial-state image of the MW sample with in colors the segmented phases. (b) Visual comparison of a "slow" events show different fluid configurations of water (light gray) and oil (black). The blue arrows indicate the movement of the brine phase. Note that the brine phase bulges into the oil-phase indicating oil-wet conditions. (c) By calculating the fluid occupancy over time for a single pore body, displacements can be identified and the duration of the event calculated.

2. Materials and Methods

To investigate fluid dynamics in complex porous media, we performed unsteady-state multiphase flow experiments in twin microcores (29 mm long, 6 mm diameter) of a heterogeneous, calcareous quarried sandstone (Luxembourg Sandstone (Molenaar, 1998)) with a multiscale pore geometry (Figure 1a, Figures S1 and S3 in Supporting Information S1). Mercury intrusion porosimetry showed that the sample had a bimodal pore throat size distribution centered on radii $R_{micro} = \sim2$ µm and $R_{inter} = \sim20$ µm for the micro- and intergranular pores, respectively (Figure S1 in Supporting Information S1). One sample was used in its native homogeneously hydrophilic state (water-wet, WW), while the wettability of the second sample was chemically altered to obtain a mixed-wettability (MW) using a protocol based on Herring et al. (2016). The alteration was performed by partially saturating the microcore with a 5 wt.% Octadecyltrichlorosilane (OTS) solution to deposit a hydrophobic coating followed by cleaning and drying the sample.

We performed oil- (OF) and subsequent waterflooding (WF) experiments using a 1.0 mol·kg^{-1} potassium iodide (KI) brine and n-decane, a flow rate of 0.0006 ml/min and at ambient temperatures. The macroscopic capillary number ($C_a = \mu v/\sigma$, where v the characteristic fluid velocity in the pores, µ the invading fluid's viscosity and σ the interfacial tension) for the flooding experiments was $\sim3\cdot10^{-8}$ using $\mu_{brine} = 0.82$ mPa/s and $\mu_{decane} = 0.84$ mPa/s and a σ of 52 mN·m^{-1} (Aminabhavi et al., 1996; Gao et al., 2017; Singh et al., 2018). Under these conditions, capillary forces would typically be assumed to dominate.

The experiments were imaged continuously using dynamic laboratory-based mCT (TESCAN DynaTOM scanner) with imaging temporal resolutions of 60 s (WW-OF, MW-WF) and 120 s (WW-WF) per image and a voxel size of 8 μm. The dynamic imaging was supplemented with higher spatial and temporal resolution imaging prior to and after each experiment (4 μm/vx for WW and 3.5 μm/vx for MW) was performed prior to and after each flooding experiment.

Each reconstructed 3D image in the time series was denoised using the non-local means filter (Buades et al., 2008), registered with the normalized mutual information algorithm (Studholme et al., 1999) and segmented by manual thresholding in Avizo 2020.2 (Thermo Fisher Scientific) to classify voxels in each image either belonging to mineral, oil or brine phase (Khishvand et al., 2016; Schlüter et al., 2014).

To quantify the timescales of individual pore-scale displacements, the pore space was divided into pore bodies separated at local constrictions using a seeded watershed algorithm on the pore space distance map PNExtract, (Raeini et al., 2017). The fluid saturation of each pore body was calculated by counting the number of segmented oil voxels within its volume at each time step. The duration of a fluid displacement event (limited by the temporal resolution) was found by identifying the start and finish times of the saturation change in a pore body, and calculating the transient time by fitting a sigmoidal function to the normalized pore occupancy (MATLAB R2018b, MathWorks) (Van Offenwert et al., 2019) (Figure 1c). Pores that changed occupancy with less than 10% were omitted from the analysis to reduce the influence of image noise. Contact angles were calculated using an automatic geometric method (AlRatrout et al., 2017).

Further details on the materials and methods can be found in the Supporting Information S1.

3. Results and Discussion

Below, we first qualitatively describe our experimental results. Then, the timescales and flow rates are quantified on a pore-by-pore basis. Next, the role of wettability on the displacements is investigated. Finally, the viscous-capillary force balance of the observed dynamics is investigated.

3.1. Qualitative Comparison of Displacement Processes

Under water-wet conditions, oil was observed to displace the brine phase in a sequence of large meniscus jumps (Movie S1). These jumps were significantly faster than the temporal resolution of the mCT imaging, thus appearing as instantaneous pore-scale displacement events in the mCT images. This conforms with the expectation that a capillary-dominated drainage process takes place as an intermittent sequence of Haines jumps at the milli-second timescale (Armstrong & Berg, 2013). In the subsequent waterflooding experiment (Movie S2), water layers were observed to slowly swell from the sides of the pores (Figure S6 in Supporting Information S1), causing the oil to become disconnected by the occurrence of sudden snap-off events in narrow constrictions of the pore space. This is typical behavior for slow imbibition in a water-wet medium with a high pore-throat aspect ratio (Singh et al., 2019), and led to significant trapping of the oil-phase.

The sample with a mixed-wettability showed a notably different behavior during waterflooding (Figure 1b; Movie S3). The majority of the displacements were filled in fast events comparable to the drainage process in the water-wet sample. However, three observations stood out. First, the front at which the displacements occurred was more compact than that of the water-wet drainage case (Figure S7 in Supporting Information S1). Second, a significant part of the pores changed fluid occupancy over a much slower timescale: it took tens of minutes rather than a single time step for a fluid meniscus to move through such a pore. The slow events occurred concurrently with the fast events in neighboring pores. These slow events typically happened in poorly connected moldic pores, that often appear to be only connected to the rest of the network by micropores below the imaging resolution. Third, the pore walls of many of these pores visually appeared to be partly water-wet and partly oil-wet (Figure 1b). We observed both events where brine moved into the center of the pore body while bulging into the oil (Figure 1b; Movies S4 and S5) and events with a near flat meniscus (Figure S6 in Supporting Information S1; Movies S6 and S7). This was distinct from layer swelling during waterflooding of the water-wet sample, where the water-layers always swelled from the smaller pores and corners.
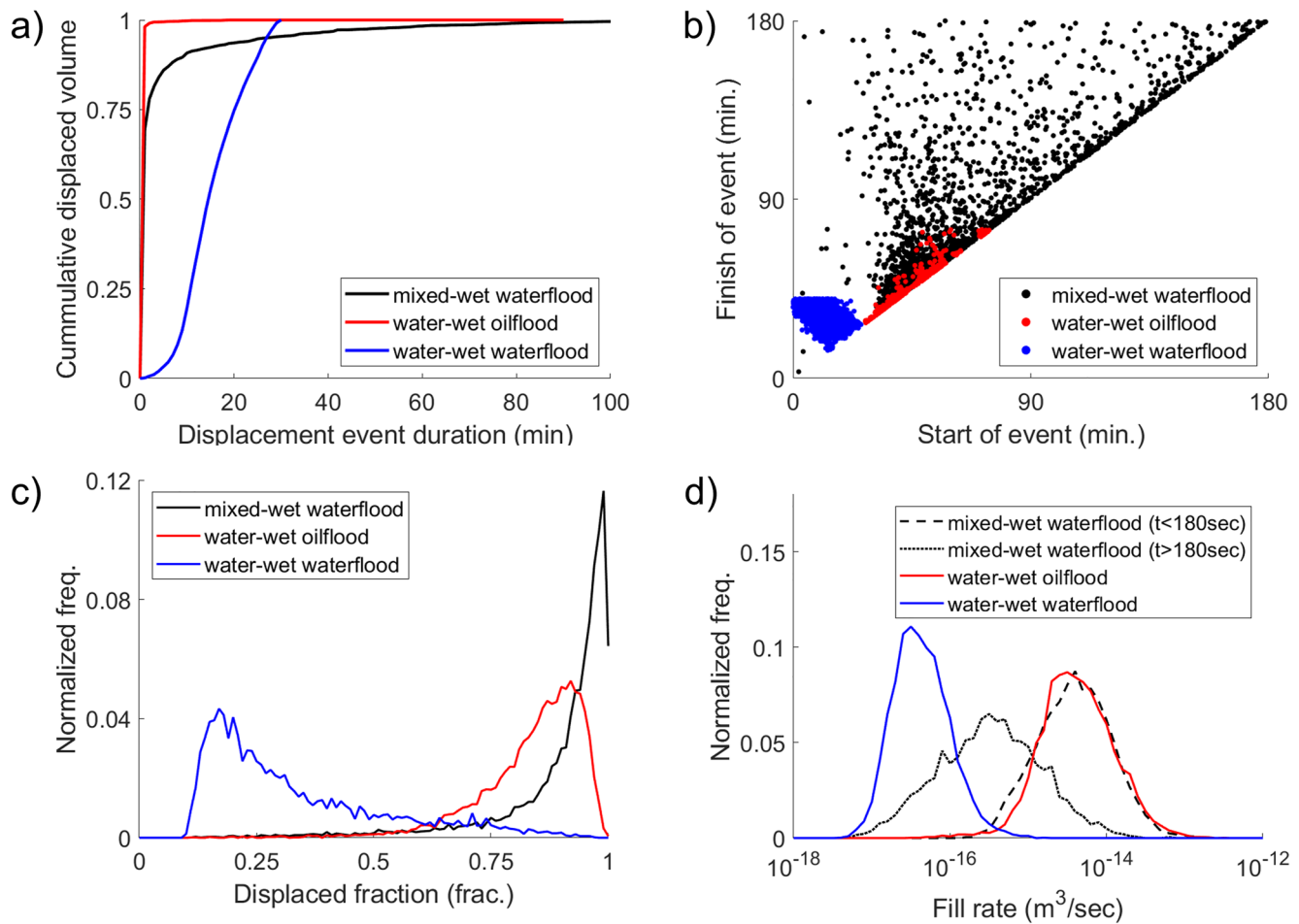
Figure 2. (a) During the waterflood in the mixed-wettability (MW) sample more than 19% of the total displaced volume of fluid occurred in events that took more than a minute to complete. (b) Start and finish times were identified on a pore-by-pore basis. (c) Waterflooding displacements under MW conditions were able to displace a substantial larger amount of defending phase within a pore body compared to the imbibition and drainage processes observed under WW conditions. (d) Distribution of effective fill rates for fluid displacement events in individual pores. The calculated effective rate or events occurring faster than the temporal resolution is a lower limit and is likely much higher. For MW conditions, events with a duration shorter than 180 s are plotted separately from those who took more than 180 s to complete.

3.2. Quantification of Pore-Scale Displacements Events

In this section, the timescales of the displacement events are quantified to relate them to the overall flow conditions and characteristics of the sample.

In the water-wet sample, 98% of the displaced volume during the oilflood was associated with pore filling events that completed faster than the temporal resolution of the imaging (Figure 2a). Longer pore filling events were associated with two or more intermittent displacements inside one pore body that each took less than one time step to complete. Displacements during the waterflood in the same sample took typically 10–20 min to complete. Note that the filling duration calculated here included the reversible swelling of wetting layers, which led up to capillary instabilities and subsequent "snap-off" redistributions of the fluids.

The displacements in the MW–WF case had a distinctively different temporal signature. While most of the fluid displacement occurred in events that took less than one time step to complete, 19% of the displaced oil volume was associated with events that took longer than 60 s. The cumulative pore filling duration distribution shown in Figure 2a has a long tail, spanning almost the full duration of the experiment. These slow fillings appeared not to be dominated by capillary forces in the same way as during a typical drainage, which would have resulted in instabilities that caused fast fluid redistribution as soon as the invasion capillary pressure of a pore throat was overcome. On average, the slow displacement events took place in pores with

lower connectivity than the instantaneous events: only 46% of the former (filling time >10 min) had at least one connection to the percolating cluster of resolved macro-pores, compared to 80% of the latter. Displacements with a long duration occurred concurrently with those that completed within one time step (Figure 2b), which shows the start and finish time of each detected displacement event. The slow filling dynamics may thus have a non-trivial influence on the order in which pores are invaded by brine, and therefore potentially on the fluid distribution patterns that arise from this (Figure S9 in Supporting Information S1).

The waterflooding process under mixed-wet conditions was found to be able to displace a larger fraction of the volume of a pore body than the drainage process in the WW sample (Figure 2c) highlighting the importance of the role of surface wetting on the overall displacement processes. It also clearly shows the distinction between the slow events in the water-wet waterflooding (due to layer swelling) and the slow invasion events in the mixed-wet waterflooding, which tended to invade the pore centers in a piston-like manner. Moreover, this may affect the energy balance of the displacement process due to differences in energy dissipation between the different displacement processes.

The rate at which fluids flow through a porous medium is closely related to the capillary-viscous force balance that control the fluid distributions. We define the effective displacement rate as the volume of displaced fluid within a pore divided by the duration of this displacement. The calculated effective displacement rates are shown in Figure 2d. These are a lower limit to the actual displacement rates due to the limited temporal resolution of the measurement. Note that the effective filling rates for a single pore were up to six orders of magnitude slower than the overall flow rate set on the pump ($1 \cdot 10^{-11}$ m³/sec).

3.3. Wettability and Pore Scale Dynamics

Wettability has a strong influence on the position of the fluid-fluid interfaces during multiphase flow and can alter the sequence in which pores are invaded in mixed-wet media (Scanziani et al., 2020). The wettability of a material is quantified by a contact angle, that can be calculated geometrically directly from 3D mCT images of fluid distributions (AlRatrout et al., 2017). Contact angles were calculated on high-resolution images of the static fluid distributions after waterflooding and are presented in Figure 3 for both samples. The mean contact angle calculated for the sample in its native state suggested weakly water-wet conditions (69°). The pore-by-pore mean contact angle varied through the pore space for the MW sample (Figure 3b), with part of the distribution below and above 90° (mean of 94°). While these contact angle distributions likely carry significant uncertainty due to the limited spatial resolution, high levels of image noise, and (to a lesser extent) due to fluid meniscus dynamics (Akai et al., 2019; Mascini et al., 2020; Sun et al., 2020), the observed shift between the distributions in the two samples indicated a shift to mixed-wet conditions in the OTS-treated sample (AlRatrout et al., 2018).

By themselves, the measured wettability properties of the mixed-wet sample did not explain the slow filling dynamics that we observed. In addition to the "static" contact angles in Figure 3a, we investigated the relation between the wettability and the dynamics by measuring the local contact angles at the start of each fluid invasion event in the dynamic imaging data (Mascini et al., 2020). Unlike contact angle measurements on static fluid distributions, which contain pinned contact lines that can yield any value between the advancing and receding contact angles, the latter "event-based" measurements indicate the contact angle at the time when fluid displacements started (Figure 3c). In our mixed-wet experiment, the event-based contact angles were very similar in fast- and slow-filling pores, as was the hysteresis between the measured contact angles at the start and end of the filling events (Figure 3d). This suggests that the time-scale of the dynamics was not controlled by the local wettability alone. Nevertheless, contact angle measurements on fast time resolved mCT data may suffer from the limited spatial and temporal resolution of these measurements. Further experiments at synchrotron facilities which offer imaging capabilities at higher resolutions are needed to confirm this.

3.4. Filling Dynamics and the Viscous-Capillary Force Balance

In the capillary limit, fluid displacement can only take place if both fluid phases are connected through the sample (i.e., there is no mobilization of trapped ganglia due to viscous forces). When connected fluid pathways become narrow, the area available for fluid flow may limit the rate of fluid displacements.
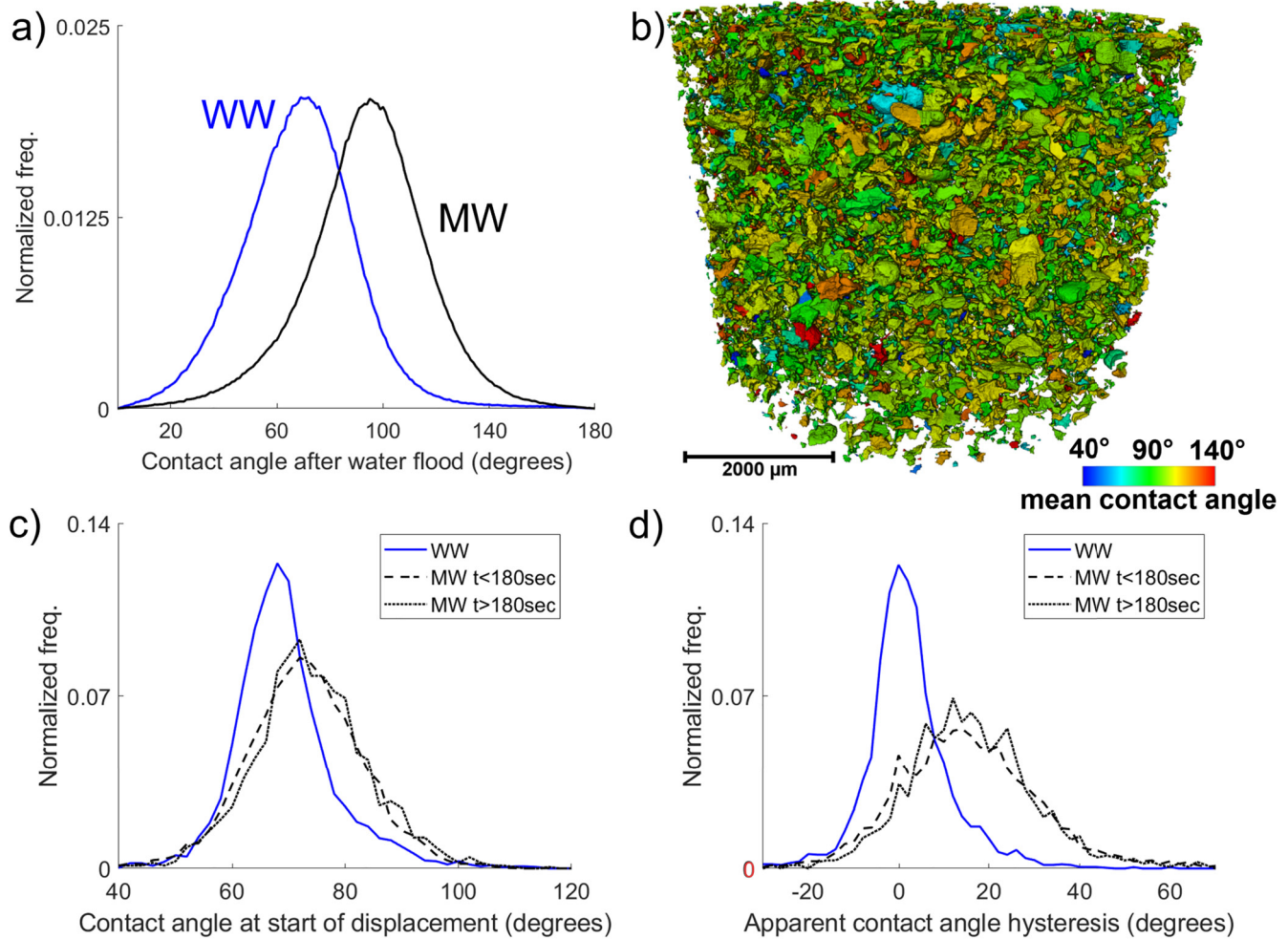
Figure 3. (a) Distributions of contact angles on static fluid distributions after the waterflood. The mixed-wet distribution shows a distribution that covers both values above and below 90 degrees which is typical for mixed-wet rocks. (b) The spatial distribution of contact angles post waterflood averaged for each pore body inside the mixed-wet sample. (c) Distribution of the mean contact angles for each pore body at the start of the displacement event calculated on the dynamic mCT data of the water- and mixed-wet data. (d) Distribution of the apparent contact angle hysteresis per pore for both water- and mixed-wet conditions during waterflooding. In both (c) and (d) there is no obvious difference in distribution between events that take less than 180 s and events that take longer to complete.

Conductivity-limited behavior has been observed indirectly during the final stages of drainage experiments in water-wet rocks (El-Maghraby & Blunt, 2013). During these final stages, the water phase is displaced via a network of thin water layers in the corners and crevices of rough pore walls. As the area available for the water phase is limited, the relative permeability is very low (orders of magnitude lower than the relative permeability of the non-wetting phase). The time it takes to reach capillary equilibrium in this case can be days for a small cm-scale sample, compared to the timescale of milliseconds of the initial Haines jumps that filled most of the pore space (Blunt, 2017). There are, however, important differences with the fluid filling events described in this work: (a) the events occur concurrently with the fast displacements in neighboring pores and (b) the events fill complete pore bodies rather than consisting of interfaces merely invading small pore corners and crevices. As such, the slow events have the potential of severely impacting the displacement sequence, and thus fluid connectivity and the resulting upscaled flow properties.

The prevalence of the slow filling events can be explained by taking into account both the wettability and the pore space architecture. Microporous materials, such as mineral cements and clays, can provide structural bottle necks between larger intergranular pores that impede fluid flow. The pore throats in these narrow structures might differ orders of magnitude with larger neighboring pores. Large heterogeneity in

the pore size promotes the loss of fluid connectivity during the invasion, due to trapping by, for example, snap-off and bypassing (Blunt, 2017). However, mixed-wet systems are known to preserve this connectivity longer than homogeneously-wetted systems (Lin et al., 2019; J. Zhao et al., 2018). As a consequence, filling events that cannot proceed in a water-wet systems, may proceed in mixed-wet systems. When this happens, narrow connections through micro-pores and wetting layers therein may cause bottlenecks in the fluids' "supply chain," thereby causing conductance-limited behavior that significantly slows down the pore-scale invasion dynamics. This likely explains why slow filling dynamics were less pronounced in previous studies of mixed-wet systems with simpler pore structures, such as Bentheimer sandstone or Ketton limestone (Rücker et al., 2019; Scanziani et al., 2020).

The local balance between viscous and capillary forces during the slow filling events can be investigated using a simple model of the pore space architecture in our experiment. We model the situation that the invading fluid had to pass through a patch of tight throat radii to invade a large pore. The flow thus passed through an intergranular pore (throat) with typical dimensions on the order of $R_{\text{inter}} \times R_{\text{inter}} \times R_{\text{inter}}$ (20 µm), which was cemented with microporous material with throat size R_{micro} (2 µm). Using respectively the multiphase extension of the Darcy equation and the Young-Laplace equation, the balance between the viscous pressure drop P_v over this blocked throat and its capillary intrusion pressure P_c is:

$$\frac{P_v}{P_c} = \frac{\mu q_{\text{local}} R_{\text{inter}}}{k_{\text{micro}} \cdot k_{\text{micro},r}} \cdot \frac{R_{\text{micro}}}{2\sigma |\cos\theta|} = Ca_{\text{local}} \cdot \frac{R_{\text{micro}} \cdot R_{\text{inter}}}{k_{\text{micro}} \cdot k_{\text{micro},r}} \cdot \frac{1}{2|\cos\theta|}$$

Where μ is viscosity, q_{local} is the local fluid flux approximated by the effective displacement rate, k_{micro} and $k_{\text{micro, r}}$ are the absolute and relative permeability of the microporosity, σ is the interfacial tension, θ is the advancing contact angle and Ca_{local} is a local capillary number defined to equal $\mu q_{\text{local}}/\sigma$. Following (Blunt, 2017), a typical permeability for the microporosity with this throat size is on the order of 10^{-15} m^2, and an average contact angle of 94° (Figure 3a, assuming a similar contact angle for the micropores). Using these values, we find that:

$$\frac{P_v}{P_c} \approx 10^5 \cdot \frac{Ca_{\text{local}}}{k_{m,r}}$$

Based on the flow rates measured in the mCT data, the typical Ca_{local} for slow pore filling events mediated by this microporous patch would be on the order of 10^{-7} (Figure S8 in Supporting Information S1). Given the fact that the relative permeability to either the invading or the escaping phase is expected to be low ($<<10^{-1}$) in a mixed-wet medium, the local ratio between viscous and capillary forces can easily approach values on the order of 1. This indicates that in samples where pore sizes differ orders of magnitude, viscous forces could play a significant role in the displacement process even at very low global capillary numbers. The mixed-wet wettability plays a crucial role here, as it allows to maintain fluid connectivity–and thus displacement processes to proceed–even for very low relative permeabilities to either of the fluids (Lin et al., 2019). Further imaging studies at higher resolutions are needed to confirm this.

4. Conclusions

One of the main open questions in the field of multiphase flow is how to link pore-scale displacements to macro-scale behavior of multiphase flow. As the underlying pore-scale displacement dynamics in water-wet and mixed-wet conditions are poorly understood, we used time-resolved microcomputed tomography to image unsteady-state multiphase flow experiments in a calcareous sandstone with a complex pore structure. The pore-scale dynamics were qualitatively and quantitative different for water- and mixed-wet conditions. Displacements during the oil-flood in the water wet-sample were associated with Haines instabilities, while corner and layer flow with subsequent snap-offs were observed during the water-flood of this sample. In the waterflooding of a mixed-wet sample, we identified a displacement mechanism during which 19% of the displaced volume was associated with displacements took longer than 60 s to complete. The slow displacement events occur concurrently with Haines instabilities occurring in directly neighboring pores and are characterized by the fluid meniscus moving through the center of the pore space.

The occurrence of viscous effects has been demonstrated experimentally for higher capillary numbers (10^{-6}–10^{-4}), in the form of intermittency (Reynolds et al., 2017), ganglion dynamics (Rücker et al., 2015) or break-up of ganglia in rocks with a multiscale pore system (Pak et al., 2015). The work presented here demonstrates that even at much lower capillary numbers ($\sim 10^{-8}$), pore-scale complexities, such as mixed-wettability and multi-scale pore geometries, can cause significant pore-scale variations in the capillary-viscous force balance. This can influence the displacement process in complex pore spaces, particularly under mixed-wet conditions. Therefore, such effects need to be considered when performing pore network modeling of multiphase flow in complex pore spaces. Our observations spur further investigation into the classification of phenomena caused by pore-scale variability in the driving forces of multiphase flow in heterogeneous porous materials. Ultimately, this may lead to better models of fluid flow in the subsurface critical for groundwater resources and CO_2 sequestration operations.

Data Availability Statement

The data described in this manuscript can be retrieved from https://doi.org/10.17612/GEN3-2P41.

References

Akai, T., Lin, Q., Alhosani, A., Bijeljic, B., & Blunt, M. (2019). Quantification of uncertainty and best practice in computing interfacial curvature from complex pore space images. *Materials*, *12*(13), 2138. https://doi.org/10.3390/ma12132138

Al-Raoush, R. I. (2009). Impact of wettability on pore-scale characteristics of residual nonaqueous phase liquids. *Environmental Science & Technology*, *43*(13), 4796–4801. https://doi.org/10.1021/es802566s

AlRatrout, A., Blunt, M. J., & Bijeljic, B. (2018). Wettability in complex porous materials, the mixed-wet state, and its relationship to surface roughness. *Proceedings of the National Academy of Sciences*, *115*, 8901–8906. https://doi.org/10.1073/pnas.1803734115

AlRatrout, A., Raeini, A. Q., Bijeljic, B., & Blunt, M. J. (2017). Automatic measurement of contact angle in pore-space images. *Advances in Water Resources*, *109*, 158–169. https://doi.org/10.1016/j.advwatres.2017.07.018

Aminabhavi, T. M., Patil, V. B., Aralaguppi, M. I., & Phayde, H. T. S. (1996). Density, viscosity, and refractive index of the binary mixtures of cyclohexane with hexane, heptane, octane, nonane, and decane at (298.15, 303.15, and 308.15) K. *Journal of Chemical & Engineering Data*, *41*(3), 521–525. https://doi.org/10.1021/je950279c

Armstrong, R. T., & Berg, S. (2013). Interfacial velocities and capillary pressure gradients during Haines jumps. *Physical Review E*, *88*(4), 043010. https://doi.org/10.1103/physreve.88.043010

Berg, S., Ott, H., Klapp, S. A., Schwing, A., Neiteler, R., Brussee, N., et al. (2013). Real-time 3D imaging of Haines jumps in porous media flow. *Proceedings of the National Academy of Sciences*, *110*(10), 3755–3759. https://doi.org/10.1073/pnas.1221373110

Blunt, M. J. (2017). *Multiphase flow in permeable media: A pore-scale perspective*. Cambridge University Press. https://doi.org/10.1017/9781316145098

Blunt, M. J., Bijeljic, B., Dong, H., Gharbi, O., Iglauer, S., Mostaghimi, P., et al. (2013). Pore-scale imaging and modelling. *Advances in Water Resources*, *51*, 197–216. https://doi.org/10.1016/j.advwatres.2012.03.003

Blunt, M. J., & Scher, H. (1995). Pore-level modeling of wetting. *Physical Review E*, *52*(6), 6387–6403. https://doi.org/10.1103/PhysRevE.52.6387

Buades, A., Coll, B., & Morel, J.-M. (2008). Nonlocal image and movie denoising. *International Journal of Computer Vision*, *76*(2), 123–139. https://doi.org/10.1007/s11263-007-0052-1

Bui, M., Adjiman, C. S., Bardow, A., Anthony, E. J., Boston, A., Brown, S., et al. (2018). Carbon capture and storage (CCS): The way forward. *Energy & Environmental Science*, *11*(5), 1062–1176. https://doi.org/10.1039/C7EE02342A

Bultreys, T., Boone, M. A., Boone, M. N., De Schryver, T., Masschaele, B., Van Hoorebeke, L., & Cnudde, V. (2016). Fast laboratory-based micro-computed tomography for pore-scale research: Illustrative experiments and perspectives on the future. *Advances in Water Resources*, *95*, 341–351. https://doi.org/10.1016/j.advwatres.2015.05.012

Bultreys, T., Boone, M. A., Boone, M. N., De Schryver, T., Masschaele, B., Van Loo, D., et al. (2015). Real-time visualization of Haines jumps in sandstone with laboratory-based microcomputed tomography. *Water Resources Research*, *51*(10), 8668–8676. https://doi.org/10.1002/2015WR017502

Chen, Y., Valocchi, A. J., Kang, Q., & Viswanathan, H. S. (2019). Inertial effects during the process of supercritical CO_2 displacing brine in a sandstone: Lattice Boltzmann simulations based on the continuum-surface-force and geometrical wetting models. *Water Resources Research*, *55*(12), 11144–11165. https://doi.org/10.1029/2019WR025746

Cieplak, M., & Robbins, M. O. (1990). Influence of contact angle on quasistatic fluid invasion of porous media. *Physical Review B*, *41*(16), 11508–11521. https://doi.org/10.1103/PhysRevB.41.11508

de Gennes, P. G. (1985). Wetting: Statics and dynamics. *Reviews of Modern Physics*, *57*(3), 827–863. https://doi.org/10.1103/RevModPhys.57.827

El-Maghraby, R. M., & Blunt, M. J. (2013). Residual CO_2 trapping in Indiana limestone. *Environmental Science & Technology*, *47*(1), 227–233. https://doi.org/10.1021/es304166u

Gao, Y., Lin, Q., Bijeljic, B., & Blunt, M. J. (2017). X-ray microtomography of intermittency in multiphase flow at steady state using a differential imaging method. *Water Resources Research*, *53*(12), 10274–10292. https://doi.org/10.1002/2017WR021736

Haines, W. B. (1930). Studies in the physical properties of soil. V. The hysteresis effect in capillary properties, and the modes of moisture distribution associated therewith. *The Journal of Agricultural Science*, *20*(1), 97–116. https://doi.org/10.1017/s002185960008864x

Herring, A. L., Sheppard, A., Andersson, L., & Wildenschild, D. (2016). Impact of wettability alteration on 3D nonwetting phase trapping and transport. *International Journal of Greenhouse Gas Control*, *46*, 175–186. https://doi.org/10.1016/j.ijggc.2015.12.026

Holtzman, R. (2016). Effects of pore-scale disorder on fluid displacement in partially-wettable porous media. *Scientific Reports*, *6*(1), 36221. https://doi.org/10.1038/srep36221

Hu, R., Lan, T., Wei, G.-J., & Chen, Y.-F. (2019). Phase diagram of quasi-static immiscible displacement in disordered porous media. *Journal of Fluid Mechanics*, *875*, 448–475. https://doi.org/10.1017/jfm.2019.504

Khishvand, M., Alizadeh, A. H., & Piri, M. (2016). In-situ characterization of wettability and pore-scale displacements during two- and three-phase flow in natural porous media. *Advances in Water Resources*, *97*, 279–298. https://doi.org/10.1016/j.advwatres.2016.10.009

Kovscek, A. R., Wong, H., & Radke, C. J. (1992). A pore-level scenario for the development of mixed-wettability in oil reservoirs. *AlChE Journal*, *39*(1072–1085), 58. https://doi.org/10.2172/10174572

Lenormand, R., Touboul, E., & Zarcone, C. (1988). Numerical models and experiments on immiscible displacements on immiscible displacements in porous media. *Journal of Fluid Mechanics*, *189*, 165–187. https://doi.org/10.1017/s0022112088000953

Lenormand, R., & Zarcone, C. (1984). Role of roughness and edges during imbibition in square capillaries. *SPE Journal*, 13264. https://doi.org/10.2118/13264-ms

Lenormand, R., Zarcone, C., & Sarr, A. (1983). Mechanisms of the displacement of one fluid by another in a network of capillary ducts. *Journal of Fluid Mechanics*, *135*, 337–353. https://doi.org/10.1017/s0022112083003110

Lin, Q., Bijeljic, B., Berg, S., Pini, R., Blunt, M. J., & Krevor, S. (2019). Minimal surfaces in porous media: Pore-scale imaging of multiphase flow in an altered-wettability Bentheimer sandstone. *Physical Review E*, *99*(6), 063105. https://doi.org/10.1103/PhysRevE.99.063105

Mascini, A., Cnudde, V., & Bultreys, T. (2020). Event-based contact angle measurements inside porous media using time-resolved micro-computed tomography. *Journal of Colloid and Interface Science*, *572*, 354–363. https://doi.org/10.1016/j.jcis.2020.03.099

Mercer, J. W., & Cohen, R. M. (1990). A review of immiscible fluids in the subsurface: Properties, models, characterization and remediation. *Journal of Contaminant Hydrology*, *6*(2), 107–163. https://doi.org/10.1016/0169-7722(90)90043-G

Molenaar, N. (1998). Origin of low-permeability calcite-cemented lenses in shallow marine sandstones and $CaCO_3$ cementation mechanisms: An example from the Lower Jurassic Luxemburg Sandstone, Luxemburg. In S. Morad (Ed.), *Carbonate cementation in sandstones* (pp. 193–211). Blackwell Publishing Ltd. https://doi.org/10.1002/9781444304893.ch9

Morrow, N. R. (1975). The effects of surface roughness on contact: Angle with special reference to petroleum recovery. *Journal of Canadian Petroleum Technology*, *14*(04). https://doi.org/10.2118/75-04-04

Morrow, N. R. (1990). Wettability and its effect on oil recovery. *Journal of Petroleum Technology*, *42*(12), 1–476. https://doi.org/10.2118/21621-pa

Mouli-Castillo, J., Wilkinson, M., Mignard, D., McDermott, C., Haszeldine, R. S., & Shipton, Z. K. (2019). Inter-seasonal compressed-air energy storage using saline aquifers. *Nature Energy*, *4*(2), 131–139. https://doi.org/10.1038/s41560-018-0311-0

Pak, T., Butler, I. B., Geiger, S., van Dijke, M. I. J., & Sorbie, K. S. (2015). Droplet fragmentation: 3D imaging of a previously unidentified pore-scale process during multiphase flow in porous media. *Proceedings of the National Academy of Sciences*, *112*(7), 1947–1952. https://doi.org/10.1073/pnas.1420202112

Rabbani, H. S., Joekar-Niasar, V., Pak, T., & Shokri, N. (2017). New insights on the complex dynamics of two-phase flow in porous media under intermediate-wet conditions. *Scientific Reports*, *7*(1), 4584. https://doi.org/10.1038/s41598-017-04545-4

Raeini, A. Q., Bijeljic, B., & Blunt, M. J. (2017). Generalized network modeling: Network extraction as a coarse-scale discretization of the void space of porous media. *Physical Review E*, *96*(1). https://doi.org/10.1103/PhysRevE.96.013312

Reynolds, C. A., Menke, H., Andrew, M., Blunt, M. J., & Krevor, S. (2017). Dynamic fluid connectivity during steady-state multiphase flow in a sandstone. *Proceedings of the National Academy of Sciences*, *114*(31), 8187–8192. https://doi.org/10.1073/pnas.1702834114

Rücker, M., Bartels, W.-B., Singh, K., Brussee, N., Coorn, A., Linde, H. A., et al. (2019). The effect of mixed wettability on pore-scale flow regimes based on a flooding experiment in Ketton Limestone. *Geophysical Research Letters*, *46*(6), 3225–3234. https://doi.org/10.1029/2018GL081784

Rücker, M., Berg, S., Armstrong, R. T., Georgiadis, A., Ott, H., Schwing, A., et al. (2015). From connected pathway flow to ganglion dynamics. *Geophysical Research Letters*, *42*(10), 3888–3894. https://doi.org/10.1002/2015GL064007

Scanziani, A., Lin, Q., Alhosani, A., Blunt, M. J., & Bijeljic, B. (2020). Dynamics of displacement in mixed-wet porous media (preprint). *EarthArXiv*, *476*(2240). https://doi.org/10.31223/osf.io/jpmvc

Schlüter, S., Berg, S., Li, T., Vogel, H.-J., & Wildenschild, D. (2017). Time scales of relaxation dynamics during transient conditions in two-phase flow: RELAXATION DYNAMICS. *Water Resources Research*, *53*(6), 4709–4724. https://doi.org/10.1002/2016WR019815

Schlüter, S., Sheppard, A., Brown, K., & Wildenschild, D. (2014). Image processing of multiphase images obtained via X-ray microtomography: A review. *Water Resources Research*, *50*(4), 3615–3639. https://doi.org/10.1002/2014WR015256

Singh, K., Bultreys, T., Raeini, A. Q., Shams, M. & Blunt, M. J. (2019). Imbibition in Porous Media: Correlations of Displacement Events With Pore-Throat Geometry and The Identification of a New Type of Pore Snap-Off. https://doi.org/10.31223/osf.io/62gfr

Singh, K., Menke, H., Andrew, M., Lin, Q., Rau, C., Blunt, M. J., & Bijeljic, B. (2017). Dynamics of snap-off and pore-filling events during two-phase fluid flow in permeable media. *Scientific Reports*, *7*(1). https://doi.org/10.1038/s41598-017-05204-4

Singh, K., Menke, H., Andrew, M., Rau, C., Bijeljic, B., & Blunt, M. J. (2018). Time-resolved synchrotron X-ray micro-tomography datasets of drainage and imbibition in carbonate rocks. *Scientific Data*, *5*(1). https://doi.org/10.1038/sdata.2018.265

Studholme, C., Hill, D. L., & Hawkes, D. J. (1999). An overlap invariant entropy measure of 3D medical image alignment. *Pattern Recognition*, *32*(1), 71–86. https://doi.org/10.1016/s0031-3203(98)00091-0

Sun, C., McClure, J. E., Mostaghimi, P., Herring, A. L., Meisenheimer, D. E., Wildenschild, D., et al. (2020). Characterization of wetting using topological principles. *Journal of Colloid and Interface Science*, *578*, 106–115. https://doi.org/10.1016/j.jcis.2020.05.076

Trojer, M., Szulczewski, M. L., & Juanes, R. (2015). Stabilizing Fluid-fluid displacements in porous media through wettability alteration. *Physical Review Applied*, *3*(5), 054008. https://doi.org/10.1103/PhysRevApplied.3.054008

Van Offenwert, S., Cnudde, V., & Bultreys, T. (2019). Pore-scale visualization and quantification of transient solute transport using fast microcomputed tomography. *Water Resources Research*, *55*(11), 9279–9291. https://doi.org/10.1029/2019WR025880

Withers, P. J., Bouman, C., Carmignato, S., Cnudde, V., Grimaldi, D., Hagen, C. K., et al. (2021). X-ray computed tomography. *Nature Reviews Methods Primers*, *1*(1), 18. https://doi.org/10.1038/s43586-021-00015-4

Zhao, B., MacMinn, C. W., & Juanes, R. (2016). Wettability control on multiphase flow in patterned microfluidics. *Proceedings of the National Academy of Sciences*, *113*(37), 10251–10256. https://doi.org/10.1073/pnas.1603387113

Zhao, B., MacMinn, C. W., Primkulov, B. K., Chen, Y., Valocchi, A. J., Zhao, J., et al. (2019). Comprehensive comparison of pore-scale models for multiphase flow in porous media. *Proceedings of the National Academy of Sciences*, *116*(28), 13799–13806. https://doi.org/10.1073/pnas.1901619116

Zhao, J., Kang, Q., Yao, J., Viswanathan, H., Pawar, R., Zhang, L., & Sun, H. (2018). The effect of wettability heterogeneity on relative permeability of two-phase flow in porous media: A Lattice Boltzmann study. *Water Resources Research*, *54*(2), 1295–1311. https://doi.org/10.1002/2017WR021443